ELSEVIER

Polymer 41 (2000) 6787–6796

polymer

Investigation of hydrothermal ageing of a filled rubber toughened epoxy resin using dynamic mechanical thermal analysis and dielectric spectroscopy

K.I. Ivanova, R.A. Pethrick*, S. Affrossman

Department of Pure and Applied Chemistry, University of Strathclyde, Thomas Graham Building, 295 Cathedral Street, Glasgow G1 1XL, UK

Received 3 November 1999; received in revised form 21 December 1999; accepted 7 January 2000

Abstract

The effect of hydrothermal cycling on the water absorption behaviour of a dicyandiamide cured silica filled rubber modified epoxy resin system is reported. The water absorption and desorption behaviour of the resin were monitored gravimetrically. Dielectric and dynamic mechanical thermal analyses were carried out on samples, selected from the batches being exposed, at times which reflect various critical points in the ageing profile. It was observed that although the saturation water uptake for the samples was independent of the hydrothermal history; the equilibrium value of the mass on desorption did depend on the hydrothermal history. Deviations from simple Fickian behaviour were observed for samples, which had undergone a previous absorption–desorption cycle. This phenomenon is interpreted as water being absorbed in the polar rubbery phase of the material and not readily released on dehydration. The dielectric data provide a clear indication of the presence of a heterophase structure in the epoxy resin and are consistent with the postulate that, whilst the initial water absorption occurs reversibly in the epoxy matrix, subsequent absorption of water into the polar rubbery phase is irreversible at 50°C, the temperature used in the study.

Keywords: Rubber modified epoxy resin; Water absorption; Dielectric spectroscopy

1. Introduction

Ingress of moisture into the adhesive bond is known to degrade the bond strength of joints or the mechanical properties of carbon fibre reinforced composites [1]. Epoxy resins are often used as structural adhesives and, when fully cured, possess relatively low impact properties. Use of dicyandiamide as a curing agent generates a polymer with a low residual hydroxyl content compared with the conventional amine cured systems. A low hydroxyl content should inherently lower the ability of the resin to absorb moisture. Previous studies [2,3] on water absorption by a range of chemically different epoxy resins have explored the influence of the number of hydroxyl groups generated during cure, the cure temperature and chemical structure on the rate of water absorption. Other factors which influence the rate of water absorption are the presence of a secondary dispersed phase and the glass transition temperature, T_g, of the finally cured matrix. Improvement of the impact properties of epoxy resins has been achieved by the addition of rubber particles [4–6]. Carboxyl terminated butadiene acrylonitrile rubber [4] (CTBN) is one of the most commonly used rubber toughening systems, because it is soluble in the uncured epoxy resin [7,8]. During the cure process the rubber phase separates forming a dispersed micron size particulate phase within the epoxy matrix. The rubber particles are very effective at toughening the epoxy resin and significantly improve the impact resistance. Fillers are also commonly added to structural adhesives to improve their mechanical properties, reduce cost and sensitivity to moisture. Silicates and silica are added to formulations as either hydrophobic, usually non-reinforcing particles or as a hydrophilic reinforcing filler particles.

Water ingress into a polymer matrix leads to a range of effects; plasticisation through interaction of the water molecules with polar groups in the matrix, creation of micro crazes through environmental stress cracking, leaching of unreacted monomer and in certain cases degradation of the resin. Relatively short times of exposure lead to more or less reversible plasticisation, producing a lowering of the glass transition temperature [9]. The extent to which T_g is depressed depends on the amount of water absorbed and is described by the free volume theory, using either the Kelly

* Corresponding author. Tel.: + 44-141-548-2795; fax: + 44-141-548-4822.

0032-3861/00/$ - see front matter
PII: S0032-3861(00)00042-2

Beuche equation [10]

$$T_g = \frac{\alpha_p V_p T_g(p) + \alpha_w (1 - V_p) T_g(w)}{\alpha_p V_p + \alpha_w (1 - V_p)} \quad (1)$$

or the Fox equation [11]

$$\frac{1}{T_g} = \frac{W_p}{T_g(p)} + \frac{W_w}{T_g(w)} \quad (2)$$

where $T_g(p)$ and $T_g(w)$ are, respectively, the glass transition temperatures of polymer and water and V_i is the volume fraction of the component, W_i is the weight fraction and α_i is the expansion coefficient; the subscripts p and w refer to polymer and water, respectively. Agreement with the Fox equation [11], implies that the water is intimately mixed with the epoxy resin, rather than existing as isolated droplets or clusters. The value of T_g can also be affected by hydrolysis of the cross-linked polymer leading to a decrease in the cross-link density [12,13] and development of two-phase structure [12].

Apicella et al. [14–16] have observed that the amount of water, taken up by an epoxy resin, depends on its hydrothermal history. Exposure to water and then drying leads to an increase in the equilibrium water uptake after each cycle. It is assumed that the water causes irreversible damage to epoxy resins in the form of microcavities and part of the water is molecularly dispersed in the polymer but a part resides in the microcavities. The subsequent growth of the cavities may occur by degradation of the resin matrix or extraction of residual by-products of the synthesis of the resin. Sodium chloride is a common impurity in epoxy resins, being liberated as a result of the reaction of epichlorohydrin with the corresponding phenol. When the voids contain an electrolyte, osmotic pressure is the driving force for their growth into microcracks and microcrazes [1].

Maxwell and Pethrick [2], using dielectric relaxation methods, have observed that water may exist as either clusters in voids or in a molecularly dispersed state within the resin matrix. The water molecules in voids exhibit a dielectric signature, which is identical to that in the liquid state of water, and are designated as 'free' water molecules. Water, which is dispersed in the matrix and is usually strongly bonded through hydrogen bonding to specific functional groups is designated as 'bound' water. Bound water tends to exhibit a dielectric relaxation process in the region of 10–100 kHz at room temperature, whereas liquid water relaxes at approximately 12 GHz. Antoon et al. [17] have found that water dispersed in the epoxy matrix is usually strongly bonded to hydroxyl groups and its absorption is completely reversible. However, Jelinski et al. [18,19] infer that the movement of water in epoxy resins is impeded, there is no free water and, surprisingly, conclude that there was no evidence for tightly bound water. Woo and Piggott [20] using dielectric experiments have suggested that in certain epoxy systems water is not bound to polar groups in the resin or to hydrogen-bonding sites. It is clear that there still remain a number of uncertainties with regards the nature of the interactions between water and epoxy resins. Long-term exposure to water can lead to loss of material by degradation due to hydrolysis, oxidation, or dehydration reactions involving loss of hydroxyl groups [21]. Comyn [1] has observed that when epoxy resins are left in water for an extended period a small residue remains after evaporation of the water, the origin of which is not clear.

This study explores using a combination of dielectric spectroscopy and dynamic mechanical thermal analysis to characterise the detailed mechanism of water ingress into a structural adhesive.

2. Experimental

2.1. Materials and sample preparation

The material used was a DGEBA based epoxy resin, rubber toughened, filled with silica and cured with dicyandiamide. The material was moulded in the form of a 105 mm diameter, 2.7 mm thick disk and cured for 30 min at 170°C and a pressure of 5.75 MPa. The initial heating rate was 5°C/min and a pressure of 1.15 MPa/min was applied to the mould after the cure temperature had reached 170°C. All of the generated disks were dried in an oven at 50°C for a month and then each disk was cut into pieces to give a sample 45×45 mm and ten samples 10×30 mm. Only samples from the same disk were used to generate each set of data presented in this paper, however results obtained from the different disks are compared.

2.2. Exposure procedure

Prior to ageing the thickness and weight of each of the samples were determined. The thickness was determined by averaging several micrometer measurements taken across the sample. The 45×45 mm samples were used for the dielectric measurements and the 10×30 mm samples were used for the dynamic mechanical thermal analysis (DMTA). The samples were aged by being exposed to deionised water in sealed jars maintained at a constant temperature of 50°C + 1°C in an electronically controlled oven. During the period of the ageing study, gravimetric measurements were performed on a regular basis and dielectric spectroscopy (DS) and DMTA measurements were carried out at selected times. The samples were removed from the container, dried superficially and cooled to ambient temperature prior to the measurements.

Sets of samples were removed from the deionised water at interval of times, reflecting critical points in the ageing profile and placed in an oven with silica gel at 50°C to allow desorption of water to occur. The loss of weight was monitored gravimetrically and the DS and DMTA studies were carried out. All samples were cooled at ambient temperature before measurements were performed.

A code, which reflects the hydrothermal history of the

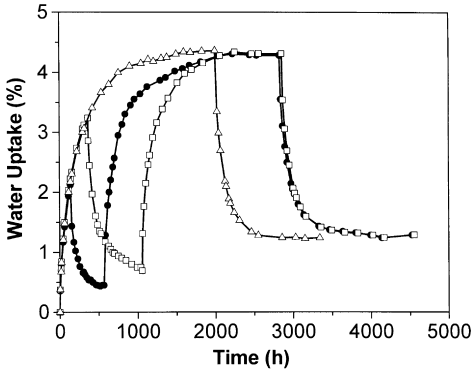

Fig. 1. Water uptake at 50°C vs. time for three different samples of the resin. Sample A (-●-) was exposed to water for 140 h and then dried in an oven, then exposed to water until saturation and dried once again. Sample B (-□-) underwent the same cycle, but for a 366 h initial exposure to water. Sample C (-△-) was exposed to water until saturation and then dried.

samples, is used to identify the data. The designates 'A' and 'B', represent:

1. initial exposure of the sample to deionised water for 140 or 366 h, respectively;
2. subsequent dehydration in an oven until no further weight loss was observed;
3. further exposure to water until saturation;
4. final dehydration until no further weight loss was observed.

The designate 'C' represents:

1. exposure to deionised water until saturation;
2. dehydration until no further weight loss was observed.

2.3. Dielectric spectroscopy measurements

Dielectric measurements were carried out using a Solatron 1250A Frequency Response Analyser (FRA) operating over the frequency range 6×10^{5}–10^{-3} Hz. The network analyser output was interfaced to the sample via an inverting amplifier and a change amplifier on the input. A standard three-terminal cell (Wayne Kerr, Type D321) was used for the measurements. The complex impedance and conductivity of the external circuit were used to calculate the dielectric permittivity ϵ' and dielectric loss ϵ''. The method used and the analysis procedures applied to the data have been discussed previously [22].

2.4. Dynamic mechanical thermal analysis

A Polymer Laboratories Dynamic Mechanical Thermal Analyser was used to measure the variation in the mechanical properties during ageing. The single cantilever mode operating at a frequency of 1 Hz was used to produce a bending deformation in the sample. The glass transition temperature was determined from the maximum in the tan δ plots. Alternative definitions can be used for the T_g based on the inflection in E' or the beginning of the drop in E'', however in this study the maximum in tan δ was the most appropriate definition.

2.5. Gravimetric measurements

The weight of the samples was determined using a Mettler AJ100 electronic balance which has an accuracy of ±0.1 mg. The times required for the weighing of the samples were considered sufficiently short for water evaporation or absorption not to be significant. The percentage water uptake was defined as the amount of water absorbed at a certain moment in time per unit weight dry polymer, multiplied by a hundred;

$$\text{Water Uptake [\%]} = \frac{W_t - W_{\text{initial}}}{W_{\text{initial}}} \times 100 \qquad (3)$$

where W_t is the weight of the sample at a certain moment of time and W_{initial} is the initial weight of the sample.

3. Results and discussion

3.1. Gravimetric analysis

The results of the gravimetric studies for water uptake at 50°C are presented in Fig. 1. The exposure of sample A to water for 140 h, resulted in an uptake of 2.1%. The sample was then dried in an oven to a constant weight and then rehydrated until saturation was achieved. Sample B was exposed to water for 366 h and took up 3.2%. The sample was then dried until it reached an equilibrium value of the weight and then re-hydrated to a saturation level. Sample C was exposed to water until it had become saturated and then dried to a constant weight. Comparison of the values of the equilibrium dry weights for the samples after the first stage of hydration depended on the period for which they were initially hydrated. The subsequent rehydration achieved a water uptake of 4.3% at saturation and a final value of 1.2% on dehydration, independent of hydrothermal history for all of the samples.

The diffusion coefficient of water into the polymer may be calculated, assuming Fickian behaviour, by plotting the water absorption/desorption as a function of the square root of time divided by the thickness of the sample. The water absorption/desorption being defined as the ratio of the amount of absorbed/desorbed water at a certain time to the equilibrium amount of sorbed/desorbed water

$$\text{Water Absorption/Desorption} = \frac{W_t - W_{t=0}}{W_{\text{equilibrium}} - W_{t=0}} \qquad (4)$$

where $W_{\text{equilibrium}}$ is the weight of the sample after equilibration and $W_{t=0}$ is the weight of the sample before the absorption/desorption.

The absorption/desorption curves, Fig. 2(a), for Sample C were fitted to the predictions of the Fickian model and good agreement between the experimental and theoretical curves were observed. The values for the diffusion coefficients

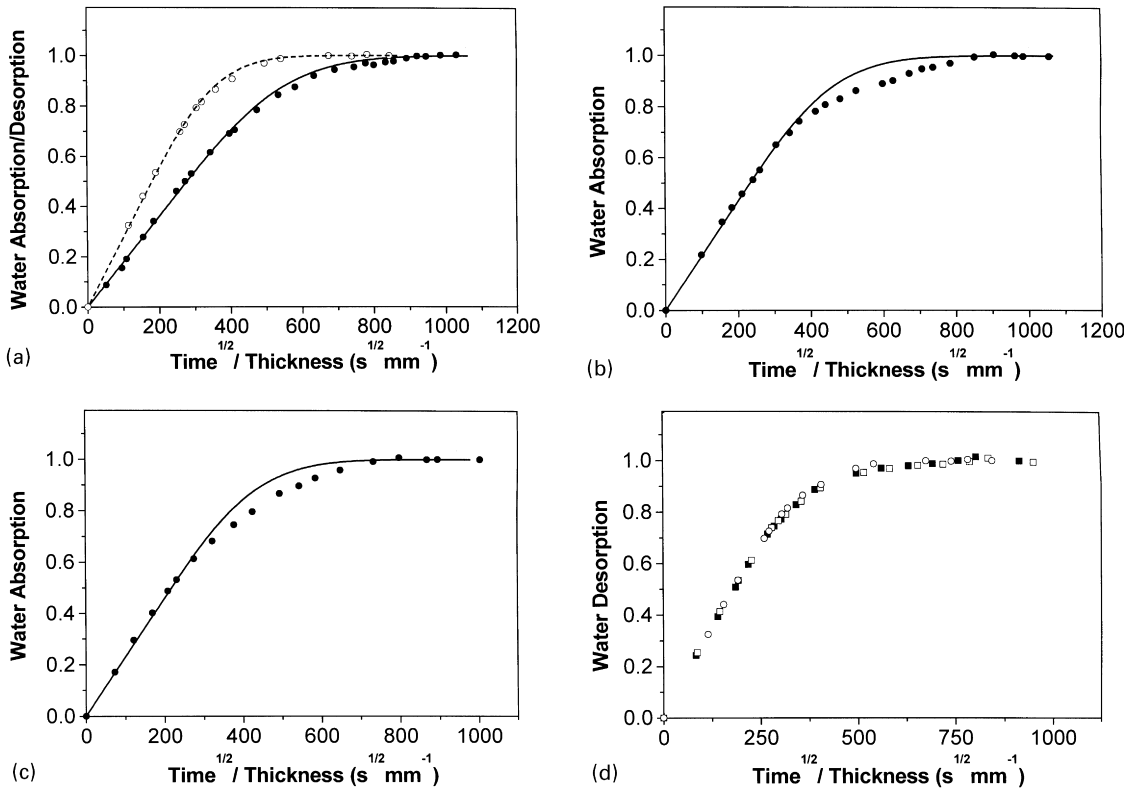

Fig. 2. (a) Water absorption (●)/desorption (○) at 50°C vs. the ratio of the square root of time to the thickness of Sample C. The lines represent the best fit to the data obtained using Fickian model for absorption (solid line) and desorption (dashed line) with diffusion coefficients 6.337×10^{-9} and 1.499×10^{-8} cm/s, respectively. (b,c) Water absorption (●) at 50°C vs. the ratio of the square root of time to the thickness of Samples A and B, respectively. The data are collected during the second exposure to water of the samples. The solid lines represent the best fit obtained with Fickian model for absorption with diffusion coefficients 8.987×10^{-9} and 9.589×10^{-9} cm/s for Sample A and B, respectively. (d) Water desorption at 50°C for Samples A (■), B (□) and C (○) after equilibration in water at 50°C.

were, respectively, $D = 6.337 \times 10^{-9}$ cm/s for absorption and $D = 1.499 \times 10^{-8}$ cm/s for desorption. The curves for samples A and B, Fig. 2(b) and (c), did not fit the Fickian model as successfully. Subsequent rehydration of the samples after being hydrated and dried resulted in a deviation from the Fickian behaviour during the rehydration process. However, if the desorption curves from all samples are compared after they have all been equilibrated, Fig. 2(d), then coincidence is once more observed between the traces.

3.2. Dynamic mechanical thermal analysis

The changes, which occur in the DMTA traces for Sample C during exposure to water, are shown in Fig. 3. A decrease in the dynamic bending modulus, E' in the glass transition region and also in the rubbery region is observed. The loss bending modulus, E'' shifts toward lower temperatures. Since E' is related to the epoxy network density [23], it appears that there is no significant loss of network structure although plasticisation of the matrix is clearly occurring. The loss factor, tan δ, changes from exhibiting a single to a double peak shape, Fig. 3(c). After 140 h of ageing, which corresponds to a water content 2.1% of the initial weight of the polymer sample, a distinct split is observed. A similar effect has been observed before and the proposed explanation was that the absorbed water is not chemically linked to the polymer network [24,25]. The water induces swelling of the material to different extents in different regions. Study of the mechanical properties of the resin during dehydration shows that this a reversible effect. As water is lost from Sample B, so the traces for E' and tan δ approach the original values for the sample, Fig. 4. Close inspection of the traces, however, reveals that although E' increases and tan δ shifts to higher temperatures, they never reach their original values. Samples A and C behave in the same manner. The longer the samples have been exposed to water the lower E', E'' and T_g after the evaporation of water. The values of the glass transition temperature at the moment when the samples have been removed from the water bath, $T_g^{(a)}$ and those after the samples have been dried to a constant weight, $T_g^{(b)}$ are presented in Table 1.

The second exposure to water of Samples A and B leads to a decrease in E', E'' and T_g and the final DMTA traces are very similar. The split in the temperature dependence of tan δ occurs at about 2.1–2.3% water content. Dehydration of the samples leads to a recovery of the DMTA trace, which is similar but not quite identical to that of the original sample. The recovery of the DMTA traces on dehydration

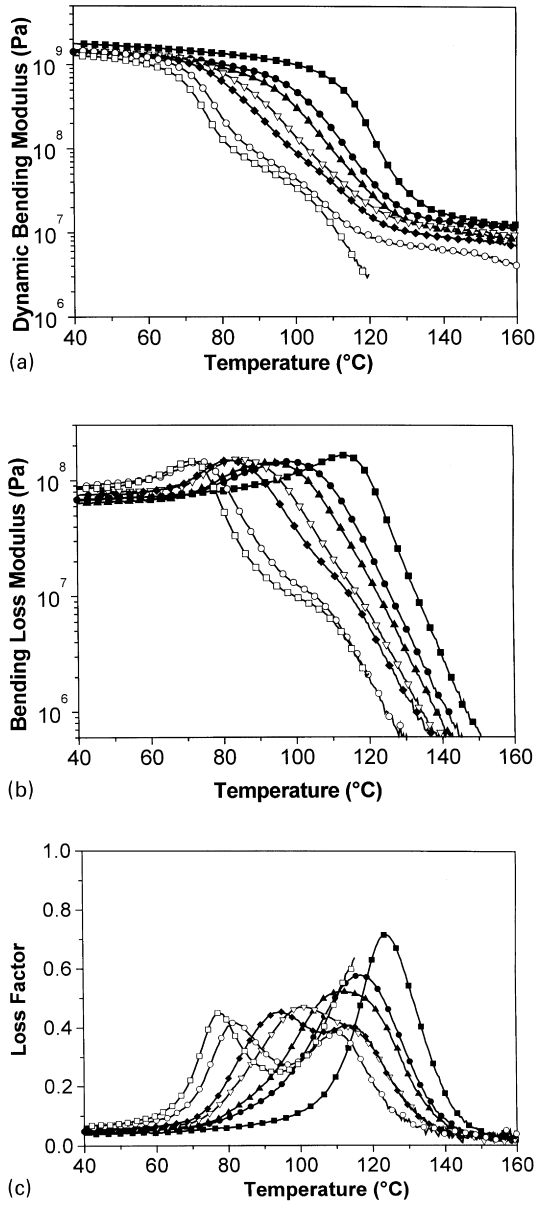

Fig. 3. (a) Dynamic bending modulus, E'; (b) bending loss modulus, E'' and (c) loss factor, tan δ, vs. temperature at different stages of ageing of Sample C. (-■-) before the start of the experiment, (-●-, -▲-, -▽-, -◆-, -○-, -□-) after ageing in water at 50°C for 22, 45, 93, 140, 400 and 2100 h, respectively.

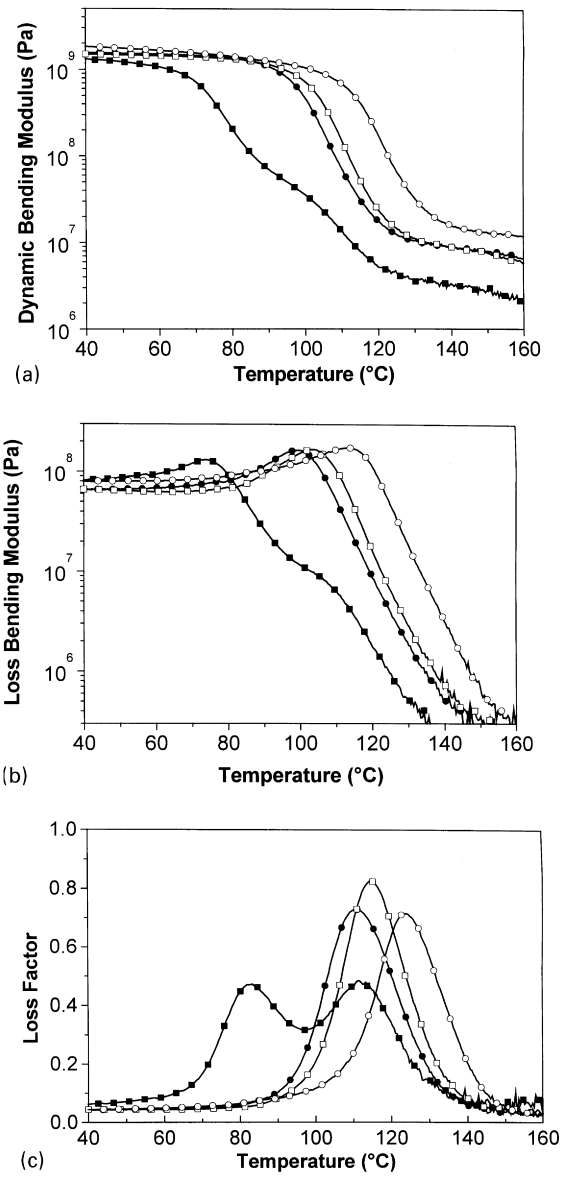

Fig. 4. (a) Dynamic bending modulus, E'; (b) bending loss modulus, E'' and (c) loss factor, tan δ, vs. temperature at different stages of dehydration of Sample B after the initial short-term exposure to water. (-■-) after 366 h in water at 50°C, (-●-) after 365 h drying at 50°C, (-□-) after 690 h, when there is no further weight loss from the sample and (-○-) before the start of the ageing process.

appears to be almost independent of the number of cycles of hydration–dehydration, Fig. 5, and is demonstrated by comparison of E' and E'' before the start of the ageing process, after the saturation in water and after the water evaporation for the three samples with different ageing history.

The absorption of water leads to a lowering of the glass transition temperature, T_g, which decreases linearly from

Table 1
Glass transition temperatures of Samples A, B and C after exposure to water at 50°C, $T_g^{(a)}$ and after drying at 50°C to constant weight, $T_g^{(b)}$

Sample	Water uptake (%)	$T_g^{(a)}$ (°C) [(K)]	Residual water (%)	$T_g^{(b)}$ (°C) [(K)]
A	2.1	95 [368]	0.45	118 [391]
B	3.2	83 [356]	0.73	115 [388]
C	4.3	77 [350]	1.24	103 [376]

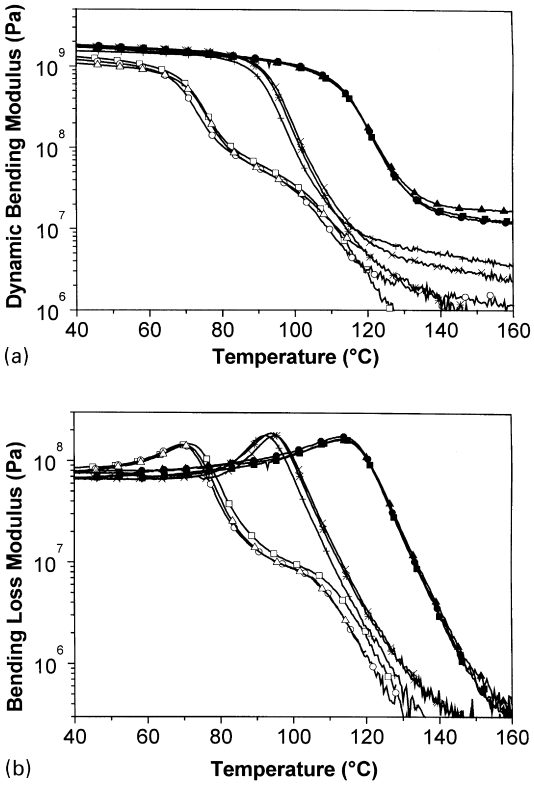

Fig. 5. (a) Dynamic bending modulus, E' and (b) bending loss modulus, E'' vs. temperature at different stages of ageing. (-■-, -●-, -▲-) represent E' and E'' of samples A, B and C before the beginning of experiment, respectively. (-□-, -○-, -△-) represent E' and E'' of samples A, B and C after saturation with water at 50°C, respectively. Finally, (-×-, -*-, - + -) represent E' and E'' of samples A, B and C after subsequent to the saturation dehydration at 50°C until no further weight loss was observed, respectively.

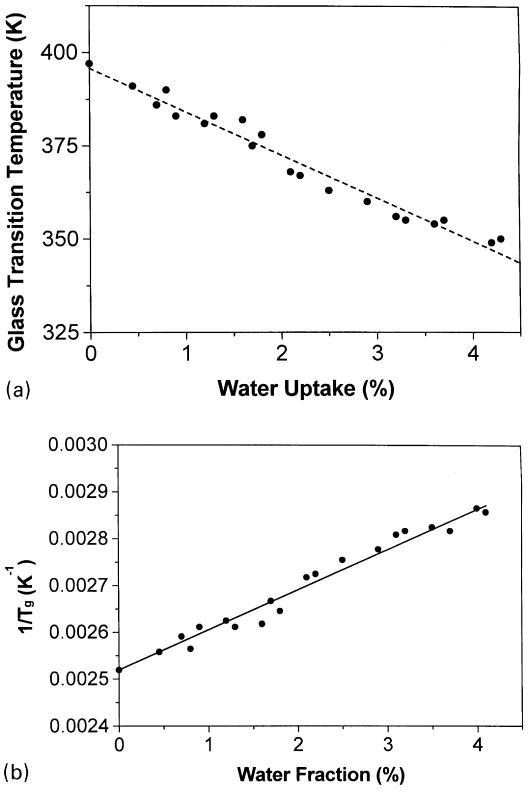

Fig. 6. (a) Glass transition temperature vs. water uptake and (b) reciprocal value of the glass transition temperature vs. water fraction. The experimental results, combined for all samples are presented by the dots, the solid line represents the best fit obtained with Fox model, where T_g of the water is 88 K.

124 to 77°C, Fig. 6(a), at a rate of 12°C per 1% of water uptake. Similar observations have been reported previously [26–30] and are interpreted in terms of plasticisation of the epoxy resin. Wright [27] found a decrease of 20°C for every 1% of water absorbed for different epoxy/hardener systems, De'Nève et al. [30] have found 8°C per 1% of water for epoxy resin based on DGEBA, cross-linked with dicyandiamide (DDA) and containing fillers (Ciba-Geigy XB3131). A plot of the reciprocal value of the glass transition temperature, T_g, as a function of the water fraction, Fig. 6(b), shows linear dependence on the water fraction as predicted by the Fox theory [12]. The solid line in Fig. 6(b) represents the best fit of the data to the Fox equation with the T_g of the water having a value of 88 K. Sugisaki et al. [31] has reported the T_g of water to be in the range 124–134 K and Hallbrucker et al. [32] has shown that T_g of the water is 136 K. It is not directly apparent why these data should predict a much lower value of the T_g of water than that found by other workers on related systems.

3.3. Low frequency dielectric spectroscopy analysis

The changes in the dielectric spectrum with time on exposure to water for sample C are shown in Fig. 7. Two distinct regions are observed. The high frequency feature (above 10 kHz) is associated with the tailing off of the process of reorientation of the pendant hydroxyl groups generated during cure [8,33]. Increases in amplitude in this region of the spectrum can be attributed to water molecules bound to the polymer chain. The lower frequency feature (below 100 Hz) could be a consequence of the heterogeneity of the matrix or/and presence of ions from impurities and water. The investigation of the nature of the high frequency process will be a subject of a subsequent publication.

On drying, the dielectric permittivity and loss of Sample C decrease with time, Fig. 8. Comparison of the curves before exposure to water with those after drying indicate that the original low values are not recovered and implies that there is a small amount of water trapped in the epoxy after drying. This is consistent with the observation of residual water after drying of the sample from the gravimetric analysis. The study of the dielectric properties of Samples A and B during the second exposure to water show similar features to those observed in the case of sample C, Fig. 9.

Fig. 10 presents the dependence of the dielectric permittivity at different frequencies on the water fraction. The results for sample C, obtained during the exposure to water are presented. The permittivities at 1 and 10 kHz

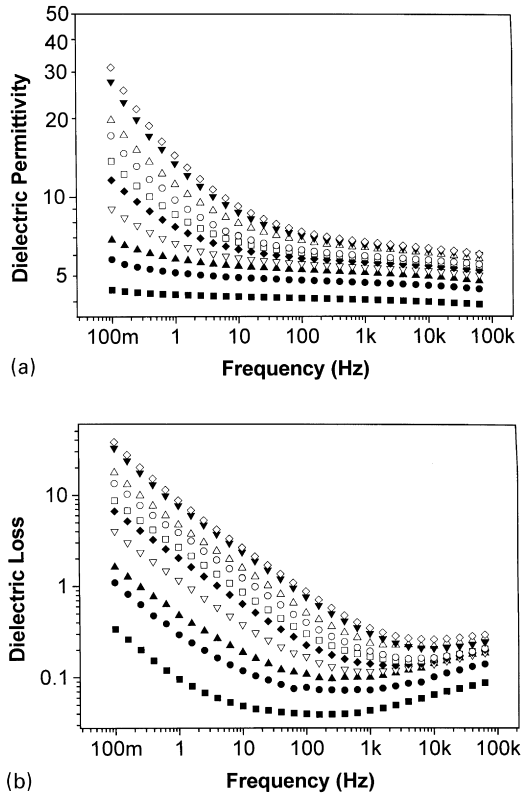

Fig. 7. (a) Dielectric permittivity and (b) dielectric loss of Sample C vs. frequency at different stages of ageing in water at 50°C. (■) dielectric permittivity and loss before the ageing, (●) those after 22 h ageing in water, (▲) after 116 h, (▽) after 159 h, (◆) after 222 h, (□) after 423 h, (○) after 536 h, (△) after 902 h, (▼) after 1209 h and (◇) after 1999 h, when no further water uptake was observed.

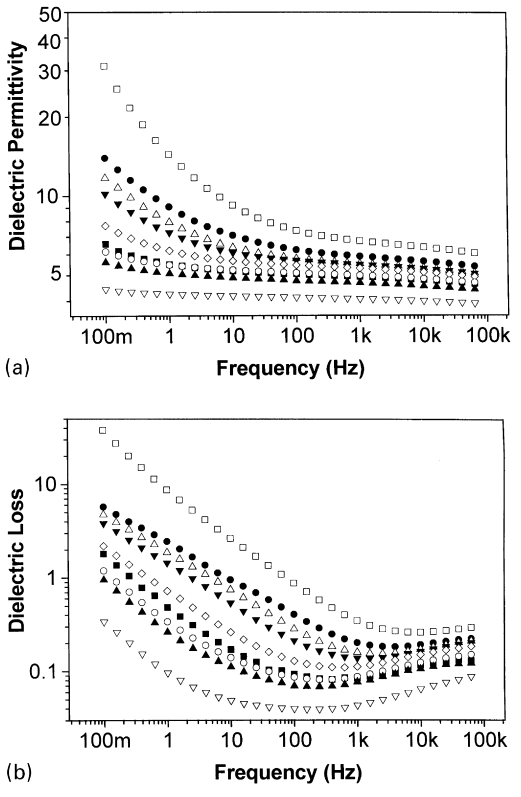

Fig. 8. (a) Dielectric permittivity and (b) dielectric loss of Sample C vs. frequency at different stages of dehydration at 50°C. (□) dielectric permittivity and loss of the resin after 1999 h exposure to water at 50°C, (●) those after 24.5 h drying at 50°C, (△) after 45 h, (▼) after 69 h, (◇) after 127 h, (■) after 242 h, (○) after 311 h, (▲) after 1342 h and (▽) permittivity and loss before the start of the experiment.

depend linearly on the water fraction in the experimental range of water fraction values, but at 1, 10 and 100 Hz the traces show deviation from linearity. The selection of 10 and 1 kHz reflects the existence of a plateau region below the relaxation of the bound water. The apparent linearity of the curves is consistent with the assumptions being made about the origins of the relaxation behaviour.

In Fig. 11(a–f) the normalised dielectric permittivity at 10 and 1 kHz is presented as a function of the ratio of the square root of time to the thickness of the sample and compared to the water absorption/desorption. The normalised dielectric permittivity, $\Delta\epsilon'$ is defined as:

$$\Delta\epsilon' = \frac{\epsilon'_t - \epsilon'_{t=0}}{\epsilon'_{\text{equilibrium}} - \epsilon'_{t=0}} \tag{5}$$

where ϵ'_t is the dielectric permittivity at a certain moment of time, $\epsilon'_{t=0}$ is the dielectric permittivity before the start of the experiment and $\epsilon'_{\text{equilibrium}}$ is the dielectric permittivity measured after the sample has reached constant weight. The traces obtained are essentially identical to those obtained by gravimetric measurements and support the assumption that the dielectric measurements are water dispersed in the epoxy resin material.

4. Conclusions

The gravimetric data indicate that, whilst the saturation level of water absorption is independent of hydrothermal history, the level of retained moisture on desorption reflects the history if saturation has not been achieved. The water uptake in the early part of the absorption study is apparently reversible, indicative of the water being primarily located in the epoxy resin. As the concentration of water increases in the epoxy resin, swelling of the matrix occurs with the observation of two peaks in the mechanical relaxation spectrum. The appearance of two peaks is indicative of heterogeneity in the structure of the material, though it is not necessarily a consequence of the rubbery phase. Unlike a fully amine cured matrix, where the cross-link density will usually be higher than a dicyandiamide cured material, swelling can induce significant changes in the polymer packing. Drying of the resin when it has been exposed to low levels of water is not quite reversible reflecting changes in the chain packing arising from the greater mobility in the swollen state. The changes in packing are manifest as a lowering in the mechanical properties after dehydration.

The residual mass retention which is consistent with water which is not released on dehydration, may be interpreted as

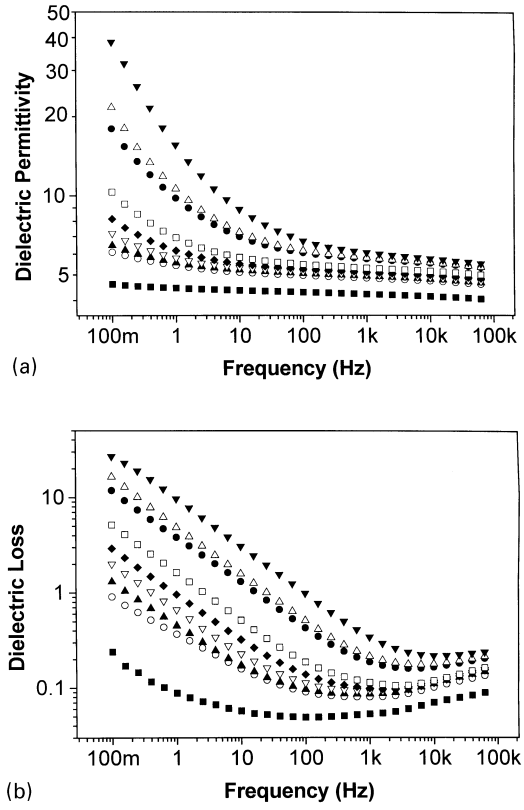

Fig. 9. (a) Dielectric permittivity and (b) dielectric loss of Sample B versus frequency at different stages of ageing in water. (■) Dielectric permittivity and loss after the sample has been exposed to water until reaching 3.2% water uptake and then dried to a constant weight (residual amount of water 0.73%), (○) permittivity and loss after 27.5 h in water, (▲) after 53.5 h, (▽) after 81.5 h, (◆) after 100 h, (□) after 142 h, (●) after 267 h, (△) 644 h and (▼) after 1801 h, when no further water uptake was observed.

being a consequence of the presence in the matrix of phase separated regions of high polarity which can effectively bind the water molecules and hence a greater enthalpy is involved in their release from the matrix. The partitioning of water between the epoxy and the polar CTBN rubber phase is only complete once saturation has been achieved. Dehydration of the samples at any point before saturation is achieved leads to a variable amount of retained water, which will depend on the volume of the CTBN in the resin, the extent to which partitioning of the water has occurred into the CTBN phase and the level of water in the epoxy phase. The water in the CTBN phase is not effectively released when the samples are dehydrated at 50°C. The retained water in the CTBN phase influences the rate of subsequent water uptake, observed as a deviation from Fickian behaviour in the gravimetric and dielectric diffusion curves.

This study has indicated that the presence of a second phase in the thermoset can influence the rate and nature of the water absorbed by a resin system. The hydrothermal effects observed in this system can be interpreted as being a consequence of the partitioning of water between the epoxy phase and the greater affinity of water for the

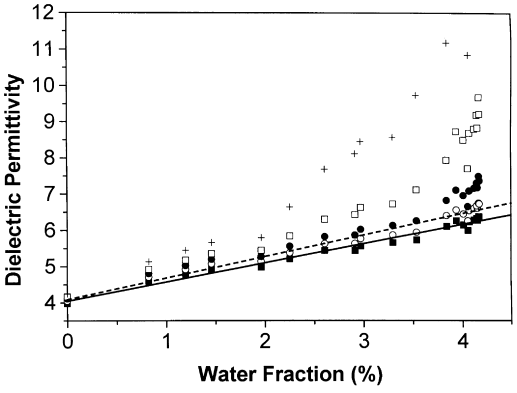

Fig. 10. Dielectric permittivity of Sample C vs. water fraction. (■, ○, ●, □, +) represent the dielectric permittivity at 10 kHz, 1 kHz, 100 Hz, 10 Hz and 1 Hz, respectively. All data are collected during the hydration of the sample.

CTBN phase. The effect of change in the composition of CTBN on the diffusion behaviour to moisture of amine cured epoxy resins has been reported recently [34] and indicates the importance of the morphology of the matrix on the observed behaviour. Significant differences in the diffusion coefficients were observed as the co-continuous phase region was approached. In this study the CTBN content is in the region when the rubber particles are dispersed in a continuous epoxy matrix and therefore anomalous behaviour would not have been expected. The characteristics for hydrated silica are currently under investigation and distinct dielectric signals have been identified. The dielectric data presented in this paper show no evidence of "specific" hydration of silica in the experiments [35]. A study of silica and silicates is currently being prepared and will be submitted for publication in the near future.

The dielectric permittivity measurements plotted against root of time, parallel very closely the data obtained by gravimetric measurement, indicating that the technique can be used on a quantitative basis to determine the water content in these materials. A plot of dielectric permittivity against weight fraction of water for frequencies above 100 Hz is linear, confirming that the dielectric permittivity can be scaled with the water content. A more detailed investigation into the basis of the correlation between the total water content and the dielectric spectrum is currently being undertaken and will form the basis of a future publication.

Acknowledgements

We wish to thank Alcan Plc (Banbury) for helpful discussion and for their support of KI in the form of a studentship for the period of this study. The assistance of Dr D. Hayward with the setting up of certain of the experiments is gratefully acknowledged.

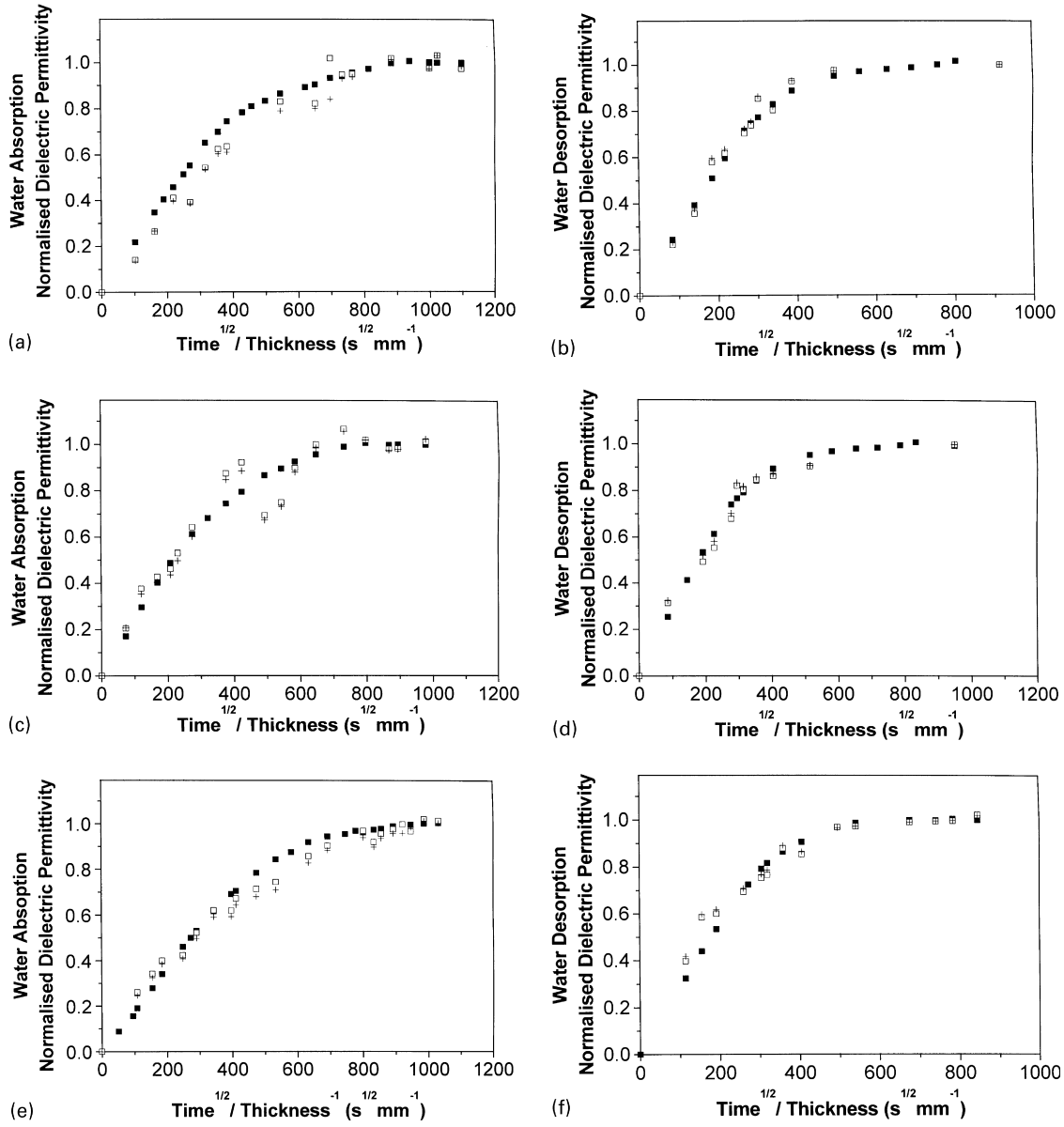

Fig. 11. Water absorption/desorption and normalised dielectric permittivity vs. the ratio of the square root of time to the thickness for Sample A (a,b), Sample B (c,d) and Sample C (e,f). The results obtained from the second hydration/dehydration cycles for Samples A and B are presented. The water absorption/desorption, and the dielectric permittivity at 10 and 1 kHz are designated (■, □, +), respectively.

References

[1] Comyn J. Polym Marine Environ 1989:153.
[2] Maxwell D, Pethrick RA. J Appl Polym Sci 1983;28:2363.
[3] Hayward D, Hollins E, Johncock P, McEwan I, Pethrick RA, Pollock EA. Polymer 1997;38(5):1151.
[4] Bucknall CB, Partridge IK. Polymer 1983;24:639.
[5] Bucknall CB, Partridge IK. Polym Engng Sci 1986;26:54.
[6] Bucknall CB, Gilbert AH. Polymer 1989;30:213.
[7] Delides CG, Hayward D, Pethrick RA, Vatalis AS. Eur Polym J 1992;28:505.
[8] Delides CG, Hayward D, Pethrick RA, Vatalis AS. J Appl Polym Sci 1993;47:2037.
[9] Li C, Dickie RA, Morman KN. Polym Engng Sci 1990;30:249.
[10] Kelly FN, Buecche F. J Polym Sci 1961;50:549.
[11] Fox TG. Bull Am Phys Soc 1926;1:123.
[12] Broutman LG. Diffusion mechanisms and degradation of environmentally sensitive composite materials. 1983, Report DOE/ER/04440-T, C00-44-0-10 (7pp.), order no. DE 83005646.
[13] Antoon MK, Koenig JL. J Polym Sci: Polym Phys Ed 1981;19:197.
[14] Apicella A, Nikolais L, Astarita G, Drioli E. Polymer 1979;20:1143.
[15] Apicella A, Nikolais L, Astarita G, Drioli E. Polym Engng Sci 1981;21:18.
[16] Apicella A, Nikolais L, Astarita G, Drioli E. Polymer 1981;22:1064.
[17] Antoon MK, Koenig JL, Serafini T. J Polym Sci: Polym Phys Ed 1981;19:1567.
[18] Jelinski LW, Dumais JJ, Stark RE, Ellis TS, Karasz FE. Macromolecules 1983;16:1019.
[19] Jelinski LW, Dumais JJ, Stark RE, Ellis TS, Karasz FE. Macromolecules 1983;18:1091.
[20] Woo M, Piggot M. J Comput Tech Res 1987;9:101.
[21] Luoma GA, Rowland RD. J Appl Polym Sci 1986;32:5777.

[22] Hayward D, Gawayne M, Mahboubian-Jones B, Pethrick RA. J Phys E: Sci Instrum 1984;17:683.
[23] Murayama T, Bell JP. J Polym Sci: Polym Phys Ed 1970;8:437.
[24] Li C, Dickie RA, Morman KN. Polym Engng Sci 1990;30:249.
[25] Xiao GZ, Delamar M, Shanahan MER. J Appl Polym Sci 1997;65:449.
[26] McKague EL, Reynolds JD, Halkias JE. J Appl Polym Sci 1978;22:1643.
[27] Wright WW. Composites 1991:201.
[28] Moy P, Karasz FE. Polym Engng Sci 1980;20(4):315.
[29] Browning CE. Polym Engng Sci 1978;18:16.
[30] De'Nève B, Shanahan MER. Polymer 1993;34(24):5099.
[31] Sugisaki M, Suga H, Seki S. Bull Chem Soc Jpn 1968;41:2591.
[32] Hallbrucker A, Mayer E, Johari GP. Philos Mag B 1989;60:179.
[33] Joshi SD, Pethrick RA, Gilmore R, Yates LW, Hayward D. J Adhesion 1997;62:281.
[34] McEwan I, Pethrick RA, Shaw SJ. Polymer 1999;40:4213.
[35] Pethrick RA, Affrossman S, Sluyk R. Unpublished work.